ELSEVIER

Biophysical Chemistry 101–102 (2002) 113–131

Biophysical Chemistry

www.elsevier.com/locate/bpc

Sequential vs. parallel protein-folding mechanisms: experimental tests for complex folding reactions

Louise A. Wallace, C. Robert Matthews*

Department of Biochemistry and Molecular Pharmacology, University of Massachusetts Medical School, 364 Plantation Street, Worcester, MA 01605, USA

Received 11 February 2002; accepted 12 April 2002

Abstract

The recent emphasis on rough energy landscapes for protein folding reactions by theoreticians, and the many observations of complex folding kinetics by experimentalists provide a rationale for a brief literature survey of various empirical approaches for validating the underlying mechanisms. The determination of the folding mechanism is a key step in defining the energy surface on which the folding reactions occurs and in interpreting the effects of amino acid replacements on this reaction. Case studies that illustrate methods for differentiating between sequential and parallel channel folding mechanisms are presented. The ultimate goal of such efforts is to understand how the one-dimensional information contained in the amino acid sequence is rapidly and efficiently translated into three-dimensional structure.

Keywords: Absorbance; Spectroscopy; Kinetics; Fluorescence

Abbreviations: Abs, absorbance; αTS, alpha subunit of tryptophan synthase; ANS, 8-anilino-1-napthalenesulfonate; CD, circular dichroism; CI2, chymotrypsin inhibitor 2; Cm, denaturant midpoint; 2′CMP, cytidine phosphate; ec, *Escherichia coli*; DHFR, dihydrofolate reductase; ESI-MS, electrospray ionization mass spectrometry; ES-MS, electrospray mass spectrometry; FL, fluorescence; GdmCl, guanidinium chloride; HX, hydrogen exchange; I, transient or stable folding intermediate; IL-1β, interleukin-1β; lc, *Lactobacillus casei*; M, monomeric state; $m^{\ddagger}$, the denaturant dependence of the transition state (‡); MTX, methotrexate; N, native monomeric state; N_2, native dimeric state; NMR, nuclear magnetic resonance spectroscopy; RNase A, ribonuclease A; SF, stopped-flow; τ, relaxation time of a chemical reaction (inverse of the rate constant, *k*); TR, wild-type *Escherichia coli Trp* aporepressor; U, unfolded state; Xaa, any amino acid

*Corresponding author. Tel.: +1-508-856-2251; fax: +1-508-856-6231.

E-mail address: c.robert.matthews@umassmed.edu (C. Robert Matthews).

0301-4622/02/$ - see front matter
PII: S0301-4622(02)00155-2

1. Introduction

The 'thermodynamic' hypothesis proposed by Anfinsen [1], that the amino acid sequence of a protein contains all of the information required to direct its folding to a unique native conformation, focuses on stable, well-defined thermodynamic states and carries the implicit assumption that the native state corresponds to the global free energy minimum. This perspective ignores the process, i.e. the dynamic response of the system, by which the reversible equilibrium between unfolded and native states shifts to accommodate to changes in environmental conditions or by which a protein folds following synthesis on a ribosome. Levinthal's paradox captures an essential aspect of the time-dependent interconversion between unfolded and native states, namely, the apparent discrepancy between the eons required for a random search and the seconds time range observed for the folding of many globular proteins [2,3]. A nonrandom search raises the possibility that the native state represents a kinetically accessible, local free energy minimum. Therefore, a complete solution of the folding problem requires kinetic studies to identify key partially folded forms and to determine the nature of the barriers on the complex, multi-dimensional energy surface that describes the folding reaction. A number of excellent reviews of this subject are available [3–12].

The formalism often adopted to analyze kinetic folding data closely follows that developed for simple chemical reactions [13]. Exponential responses are assumed to represent barrier-crossing events by populations of molecules. However, diffusive motions of the polymer chain through solvent, i.e. the Kramers formalism [14], are likely to be a more accurate description of the process than the simple vibrational motions expected for the rupture or formation of a covalent bond, i.e. the Eyring hypothesis [15]. The relatively simple reaction coordinate for chemical reactions, e.g. the length of the bond to be broken or formed, leads to predictions of rare, but essential high-energy states that serve to enhance the formation of product. The exceedingly complex reaction coordinates for protein-folding reactions currently make such predictions very difficult, leading some theoreticians to suppose that folding intermediates are a consequence of local free energy minima and may actually impede access to the native conformation [16–18].

The complexity of a reaction coordinate that attempts to describe the concerted formation of dozens, if not hundreds, of noncovalent interactions and the inherently dynamic nature of linear polymers has led to the 'new view' of the folding reaction [5,16,19–21]. In this view, folding is envisioned to involve ensembles of structures that interconvert on a highly multi-dimensional energy surface. The concept of a single folding pathway, i.e. the 'old view', is replaced by alternative trajectories for different members of the ensemble. In the limit of a completely smooth energy surface, a biased random walk [22] could result in an almost infinite number of 'pathways'.

Experimental findings have illustrated that a model between these two extremes best describes the folding properties observed for the vast majority of protein systems. With perhaps only a single exception [23], folding is a barrier-limited process that results in an exponential or multi-exponential response to a rapid change in the position of the equilibrium between stable thermodynamic states [4,8–10,12,24–27]. Although some small proteins (<100 amino acids) or stable domains of larger proteins fold via a single exponential process (for a review see Ref. [28]), the folding reaction for most proteins involves two or more such processes. The implied roughness of the energy surface can be framed in terms of classical kinetic mechanisms as a means of simply and quantitatively describing the time-dependent interconversion between the stable states. A unified view of protein folding is now emerging as a consequence of both theoretical and empirical studies [11,21].

Smooth energy surfaces have been used to describe the fast, two-state folding of proteins such as the cold shock proteins [29,30] and chymotrypsin inhibitor 2 (CI2) [31], and rough energy landscapes have been used to describe multi-state folding with transient intermediates observed for many proteins such as ribonuclease [32], α-lactalbumin [33], lysozyme [34,35], dihydrofolate reductase (DHFR) [36–40], the alpha-subunit of

Trp synthase [41–43], dimeric Trp repressor [44–49], and the heterodimer luciferase [50].

If the native and unfolded thermodynamic states are each assumed to be a manifold of microstates that interconvert far more rapidly than the reestablishment of equilibrium between these end states, the observation of two or more phases implies a set of sequential reactions. If the native and/or unfolded thermodynamic states consist of two or more slowly interconverting forms, the possibility of parallel (un)folding channels arises if (un)folding is faster than interconversion. Parallel channels could also arise if alternative substructures appear independently during the early stages of folding. Although a sequential mechanism is intrinsically simpler (and, therefore, should be tested initially), experimental evidence and the landscape view of folding both support the notion that parallel channel mechanisms must also be considered.

An analytical approach for elucidating simple kinetic folding mechanisms has been applied to lysozyme [51] and apoflavodoxin [52]. Because the dynamic response for both proteins is biphasic, three species are required to define the mechanism. The fitting of the denaturant dependences of the unfolding and refolding reactions to analytical solutions enables the different folding scenarios to be distinguished. In these cases, the observation of the entire refolding and unfolding processes, i.e. the amplitudes and relaxation times obtained at the different denaturant concentrations, provides sufficient information to discriminate among the possible mechanisms and to calculate the four independent microscopic rate constants. A triangular mechanism is the minimal model for lysozyme while the minimal model for apoflavodoxin is a linear mechanism that involves an off-pathway intermediate linked to the unfolded state (U).

Although the analytical approach provides a rigorous and exhaustive test of potential kinetic models, it is difficult to apply unambiguously to complex folding reactions, i.e. those that exhibit more than two phases. Faced with this challenge, experimentalists have devised a number of empirical tests that have the potential to highlight crucial features of a reaction and, thereby, enable the rejection of incorrect models. This review will catalog various experimental approaches that have been developed to ascertain the folding mechanisms of a variety of proteins, with a particular slant towards distinguishing between sequential and parallel mechanisms.

2. General approaches employed to study protein-folding reactions

The practical aspects of elucidating protein-folding mechanisms have been reviewed [24,25,53–55]. A minimal requirement for a mechanistic analysis is that the folding reaction must be highly reversible following denaturation, i.e. the complete recovery of the native conformation after the disruption of most, if not all, of the secondary and tertiary structure. Urea, guanidine hydrochloride, pH and temperature are typically employed as denaturants. The analysis is enhanced if the unfolding transition is monitored by a variety of structurally sensitive techniques that enable data collection over the microsecond to kilosecond time range. These techniques usually include absorbance (Abs) and fluorescence (FL) to follow the formation/disruption of tertiary structure and far-UV circular dichroism (CD) to monitor secondary structure. All three optical methods have been interfaced to commercially available stopped-flow (SF) instruments with deadtimes of 5 ms or less; ultrafast, continuous-flow instruments with deadtimes of 50 μs are being developed [56,57]. Laser-induced temperature-jump systems provide access to the nanosecond time range [58] and pressure-jump systems to the microsecond time range [59]. The possibility of residual structure in the temperature and pressure denatured states [60] suggests caution in comparison to chemical denaturation results.

The equilibrium unfolding transition provides a necessary framework for kinetic studies, both by providing constraints on the thermodynamic parameters predicted from the rate constants and by guiding the choice of conditions to favor desired states or the transitions between them. The thermodynamic parameters are most often obtained from chemical denaturation experiments by assuming that the free energy difference between the stable states depends linearly on the denaturant

concentration [61,62]; other models have also been employed [25].

By choosing strongly unfolding or refolding conditions defined by these equilibrium studies, the kinetic analysis can be simplified by neglecting the very small rate constants for the back reactions. The relaxation times for jumps into the transition zone reflect contributions from both unfolding and refolding reactions, providing further constraints for a global analysis [42]. Kinetic simulations of the experimental data are routinely performed using packages such as KINSIM [63,64] and global analysis can be done with available software, e.g. FITSIM [64] and Savuka [42]. These simulations and fitting programs enable tests of proposed folding mechanisms and the exclusion of those that are not consistent with all of the data.

3. Experimental approaches to discriminate between sequential and parallel folding mechanisms

3.1. Multiple probes of structure and function

The application of a variety of probes of secondary and tertiary structure to monitor unfolding/refolding kinetics has proved to be useful in distinguishing between parallel and sequential mechanisms. In sequential folding mechanisms, it is expected that the relaxation time of each folding event should be the same when monitored using two different probes, given that each reaction can be detected with both probes. If the observed relative amplitudes of the different events are independent of the probe then the kinetic phases may result from parallel pathways between multiple unfolded species and a common native state. In this test, the experiments are performed under conditions that favor native state formation (i.e. under strongly refolding conditions) so that the interconversion between the different unfolded species is slower than the rate of folding. This test has proved useful in distinguishing sequential and parallel mechanisms for cytochrome *c* [65], barstar [66], ribonuclease A (RNase A) [67] and lysozyme [35].

3.1.1. Case study

Cytochrome c: The refolding of yeast iso-2 cytochrome *c* displayed two slow refolding events: the slower ($\tau = 100-200$ s) of the two reactions was observed only by Abs spectroscopy while the faster event (10–20-fold faster) was observed using FL spectroscopy. Double-jump assays (Section 3.5) demonstrated that the two sets of slow folding species were formed at different rates under unfolding conditions. The fact that one of the slow events is detected by Abs and the other by FL supported the presence of structurally distinct intermediates that are each components of two parallel folding channels; the native state can also be formed directly from one of the three kinetically (but not structurally) distinct unfolded state [65,68].

3.2. Lag phase in native state formation

It is often assumed that partially folded states are essential to the formation of the native state [27,69,70] because they decrease the size of the conformational space that must be searched. However, both theoreticians and experimentalists have challenged this view because a number of small proteins (<100 amino acids) appear to attain the native fold without the participation of intermediates. Even when intermediates are detected, the issue remains whether they are on-pathway, i.e. productive and obligatory to the formation of the native state ($U \leftrightarrow I \leftrightarrow N$) or off-pathway, i.e. non-productive and slow down the folding to the native state ($I_{off} \leftrightarrow U \leftrightarrow N$). A review describing the influence of on- and off-pathway intermediates on the observed folding kinetics has appeared [19].

3.2.1. Approach

The observation of a lag phase that represents the formation of an intermediate state prior to the formation of the native state requires that the intermediate should be formed on a relatively short timescale (rapid compared to the formation of the native state) and that it should be well populated, i.e. relatively stable compared to the unfolded state. For a simple three-state mechanism ($U \leftrightarrow I \leftrightarrow N$), the magnitude of the lag period depends on the ratio of the two folding rate constants, k_{UI} and

k_{IN}. Jennings et al. [71] have provided kinetic simulations to illustrate how the observation of a lag phase is influenced by the relative relaxation times of the two folding events.

Although the typical optical methods are not well suited for detecting a lag phase, the detection can be enhanced through the use of probes that are only sensitive to the formation of the native state, e.g. ligand-binding or catalytic function. Examples of this approach include RNase A [67], DHFR [36,38,72] and interleukin-1β (IL-1β) [73], in which lag phases have been detected by double-jump assays, ligand-binding experiments and HX-ESMS, respectively. The obligatory nature of a set of intermediate states in DHFR was established using the tight binding ($K_d < 1$ nM) properties of the competitive inhibitor, methotrexate (MTX). The difference Abs spectrum of MTX bound to DHFR, with a maximum at 380 nm, makes it a selective probe of the formation of the active site cleft of DHFRs [36–38]. A distinct lag phase in Abs at 380 nm that persists for several hundred milliseconds reflects the formation of a set of intermediates that cannot bind inhibitor and whose formation could be independently detected by intrinsic tryptophan FL. Double-jump unfolding assays of the slow folding kinetics of RNase A [67] demonstrated that the formation of fully folded native protein is characterized by an initial lag period that reflects the formation of intermediates along two parallel folding channels.

3.2.2. Case study

Interleukin-1β: IL-1β, an all-β sheet protein, provided an excellent system for observing a lag phase and assessing the obligatory nature of an intermediate [73]. SF FL-detected refolding of guanidinium chloride (GdmCl)-denatured IL-1β was biphasic. The change in FL intensity with time was non-monotonic, i.e. the intensity increased rapidly ($t = 126$ ms) beyond the value expected for the native system and then decreased ($t = 42$ s) to the intensity expected for the native state at equilibrium. These results implied the presence of a spectroscopically distinct and highly populated intermediate that is formed orders of magnitude more rapidly than the native state.

Hydrogen exchange (HX) pulse labeling of the backbone amide protons, analyzed using electrospray ionization mass spectrometry (ESI-MS), ([74–79] and Section 3.7), was used to determine whether this intermediate is on- or off-pathway and to follow the time course of the formation of the native state. The kinetic rates obtained from ESI-MS were consistent with those obtained using FL and far-UV CD [80], supporting a simple sequential folding mechanism (Section 3.1). The HX-ESI-MS data showed that an intermediate with 20 protons protected from solvent–isotope exchange was formed within the first 100 ms. The intermediate was long-lived and maximally populated (~75%) for approximately 10 s. The native state only began to appear 400 ms after initiation of the refolding reaction. The lag phase in the production of the native state, while the intermediate accumulates, is consistent with the formation of an obligatory intermediate on a sequential folding pathway. Fig. 1a shows the fractional population of the different species (U, I and N) as a function of the refolding times. The partial protection of the intermediate species from exchange is consistent with a sequential mechanism with the incremental formation of structural elements in an on-pathway intermediate. Alternative mechanisms could also describe the observed optical data; however, kinetic simulations performed using KINSIM (Fig. 1b) were only consistent with a simple sequential mechanism in which the formation of native IL-1β proceeds through an obligatory intermediate.

3.3. The Initial Conditions Test

3.3.1. Approach

The observation of at least two kinetic phases in unfolding (or refolding) could be explained either by a sequential model with an on- or off-pathway intermediate or by a parallel channel mechanism with two stable native (or unfolded) forms that interconvert more slowly than they unfold (or fold). The Initial Conditions Test relies on the fact that the relaxation times for the reactions depend only on the final conditions while the amplitudes depend on both the final and initial conditions [25,32]. To test for the possibility of

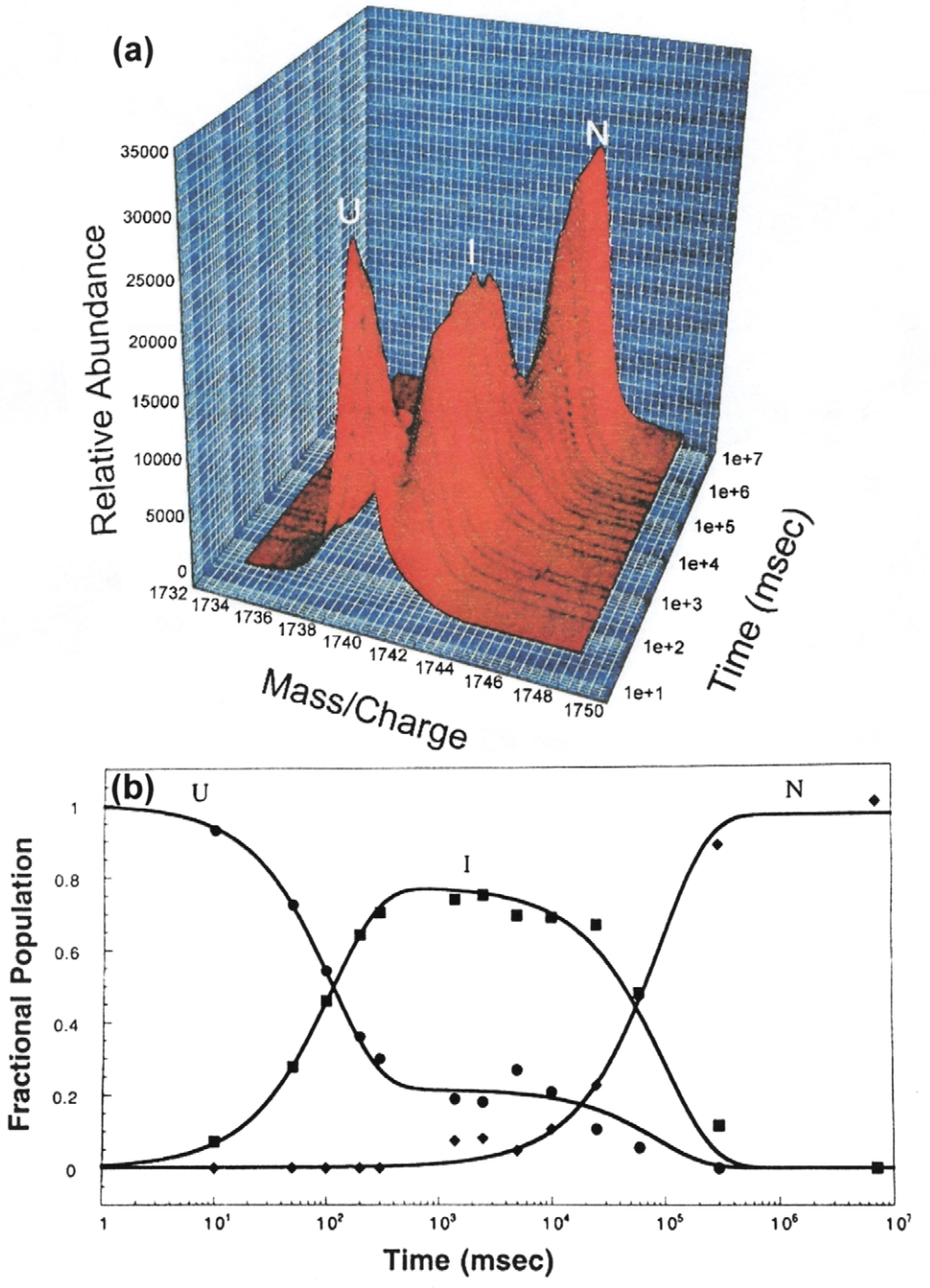

Fig. 1. Lag phase in native state formation. (a) Three-dimensional plot of the relative abundance of the observed species of IL-1β as a function of the mass/charge ratio and folding time prior to the application of the labeling pulse. (b) Plot of the fractional population of the unfolded (●), intermediate (■) and native (♦) species as a function of refolding time prior to the application of the labeling pulse. The lines represent the simulations of the mechanism proposed using KINSIM [63,64] and are compared to the experimental data. (Reprinted from Ref. [73], by permission of the publisher Nature.)

two or more stable native (or unfolded) conformations, samples are equilibrated at different starting denaturant concentrations in the native (or unfolded) baseline region. The unfolding (or refolding) reaction is initiated by rapidly transferring each sample to identical unfolding (or refolding) conditions. The resultant unfolding (or refolding) reaction traces are fitted, and the rates and amplitudes obtained from the fits are compared to those obtained for the unfolding (or refolding) of a sample maintained in the absence (or presence) of denaturant. This comparison provides important information: (i) equivalent rate constants insure that the system is behaving as expected, and (ii) the relative amplitudes provide a direct measure of the fraction of molecules that were present at the start of the reaction [32].

Because the amplitudes of the kinetic phases are proportional to the population of the species involved, the urea dependence of these amplitudes can serve to discriminate between sequential and parallel mechanisms. For example, a decrease in the amplitude for the initial, (presumably) faster event and a concomitant increase for a subsequent slower event at increasing initial denaturant concentrations would be consistent with a sequential unfolding model. The simultaneous decrease in both of the amplitudes, with midpoints near the urea concentration corresponding to the equilibrium unfolding transition, suggests that the unfolding reactions occur in parallel.

This approach has been applied to a number of systems, e.g. RNase A [32], cytochrome *c* [65], and DHFR [36]. In the case of DHFR, a shift in the equilibrium between two native states was achieved by the changing the salt concentration. The presence of 0.4 M KCl prior to unfolding resulted in the observation of only one unfolding phase. The loss of a phase is consistent with either a shift in the $N_1 \leftrightarrows N_2$ equilibrium or an increase in the rate of interconversion between the different native states. It is noteworthy that the presence of multiple native conformers of DHFR is well-documented [81–85]. A similar approach has also been applied to probe the heterogeneous nature of the unfolded state of cytochrome *c* [65]. In this case, the fraction of molecules that give rise to slow refolding phases were monitored and found to be independent of the initial denaturant conditions, suggesting that the heterogeneity of the unfolded state arises from proline isomerization. As originally proposed by Brandts et al. [86], the source of this heterogeneity can be *cis*/*trans* isomerization of the peptide bond preceding proline residues.

3.3.2. Case study

The alpha subunit of tryptophan synthase: The urea- [42,43,87–91] and GdmCl-induced [92,93] equilibrium and kinetic folding properties of alpha subunit of tryptophan synthase (αTS), a 29 kDa α/β barrel protein, display a number of complexities. The urea-induced equilibrium unfolding of αTS is multistate; two stable intermediates are highly populated at 3 and 5 M urea and are denoted as I1 and I2, respectively [42,94]. The proposed kinetic mechanism is based on an extensive and multi-faceted approach that involved several classical kinetic experiments combined with global analysis of both the unfolding and refolding kinetic data [95]. αTS is thought to fold via multiple parallel channels, and each channel involves a sequential set of native, intermediate and unfolded forms. The initial stages of folding involve an off-pathway intermediate that is populated within 5 ms and that subsequently unfolds in the hundreds of milliseconds time range to produce a set of I1-like on-pathway intermediates. The latter part of the folding response is described by three urea-independent phases that have lifetimes of 10, 40 and ~300 s in the native baseline region at pH 7.8 and 25 °C. The unfolding reaction is well-described by two kinetic phases whose relaxation times decrease exponentially with urea concentration; the lifetimes at 6 M urea are 10 and 100 s.

Although a number of different approaches were used to demonstrate the validity of the parallel mechanism for αTS, only the results from the unfolding (Fig. 2a) and refolding (Fig. 2b) jumps from various initial denaturant concentrations to the same final conditions will be discussed. The biphasic unfolding reaction raised the issue of whether the second phase originates from the formation of an intermediate state, i.e. a sequential mechanism, or from the presence of two native conformers of αTS, i.e. a parallel mechanism. The

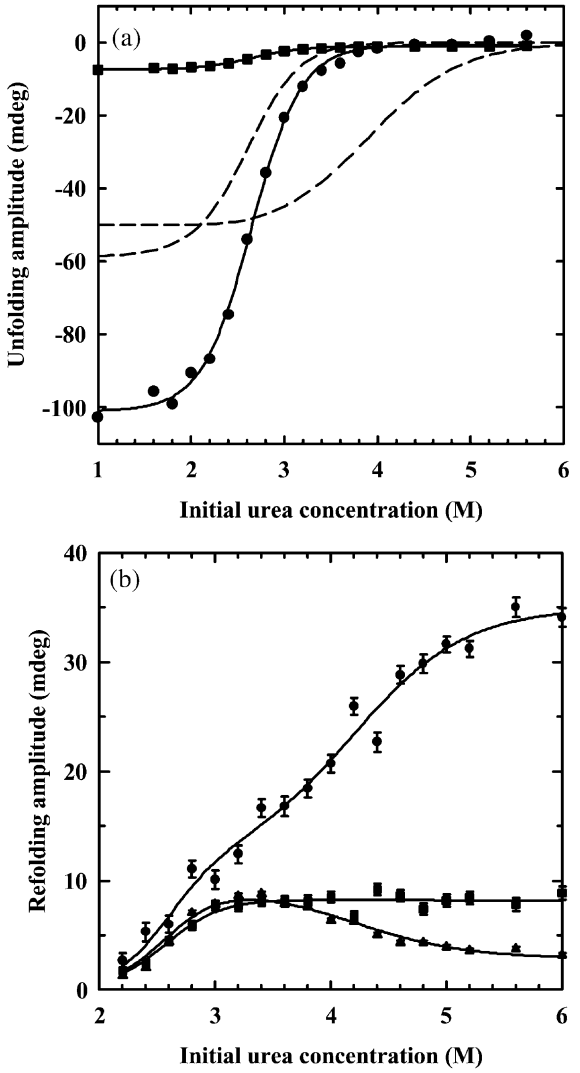

Fig. 2. The Initial Conditions Test. (a) Unfolding of αTS to 6 M urea from varying initial urea concentrations. The unfolding amplitudes of both kinetic phases are superimposed as a function of the unfolding amplitudes. Symbols represent the amplitude of the fast (circles, t = 13.7 s) and the amplitude of the slow unfolding (squares, t = 38 s) phases. The dashed lines represent the amplitudes expected if the unfolding followed a sequential mechanism. (b) Refolding of αTS to 0.6 M urea from varying initial urea concentrations. The refolding amplitudes of the 10 s (circles), 40 s (squares), and ~300 s (triangles) are shown superimposed as a function of initial urea concentration. The solid lines represent the fit to a three-state denaturation model. (Figure was taken from Ref. [42].)

amplitudes recovered from the unfolding reactions from various initial conditions (1.4–5.6 M urea) to a final concentration of 6 M urea (Fig. 2a) were best described using a two-state model, with the midpoint of the profiles (~3 M urea) of both reactions corresponding closely to the N⇆I1 equilibrium transition. The absence of a transition corresponding to the unfolding of the I1 intermediates favors the interpretation that the unfolding of a minor native-like species, occurring in parallel with a dominant native form, gives rise to the slower unfolding reaction. The amplitudes for the three refolding phases from various initial conditions (2.4–6 M urea) to a final concentration of 0.6 M urea are shown in Fig. 2b. The amplitudes show a complex dependence on the starting denaturant conditions. The amplitude for the 40 s phase increased in a sigmoidal fashion while the amplitude for the 300 s event and 10 s event displayed inflections that were indicative of three participating species. All three amplitudes have a midpoint that corresponds to the N⇆I1 transition, and the 10 and 300 s events have a second midpoint that is very similar to the I1⇆I2/U transition (because I2 and U are spectroscopically similar, they can be treated as a single thermodynamic state). These results provided further evidence for the presence of multiple intermediate states.

These findings, when combined with those from other approaches, were interpreted in terms of a kinetic model for αTS that involves four slowly interconverting unfolded forms that collapse in the millisecond time regime to form a presumed set of marginally stable intermediates with significant secondary structure. This set of intermediates are off-pathway species that must unfold to form a set of four on-pathway intermediates that correspond to the equilibrium intermediate populated at 3 M urea. All the conformers re-equilibrate to form the pair of native states via two parallel channels. The heterogeneous nature at all levels of the pathway is proposed to result from *cis*/*trans* peptide bond isomers adjacent to several proline residues [42,93]. The sensitivity of the two slower refolding events to cyclophilin, a peptidyl–prolyl isomerase, confirms the source of these two phases. Extensive site-directed mutagenesis of αTS is underway to identify the specific proline residue(s) that result

in the different folding channels (Wu and Matthews, manuscript in preparation).

3.4. The Chevron Analysis Test

3.4.1. Approach

The Chevron Analysis Test requires the complete characterization of the denaturant dependence of the unfolding and refolding relaxation times as well as their amplitudes. The logarithms of the observed relaxation times (or their reciprocals, the observed rate constants) are plotted as a function of denaturant concentration. For typical folding reactions, the pattern resembles an inverted 'V'-shape (or normal 'V'-shape) and has, therefore, been termed a chevron plot [25,54]. This shape reflects the acceleration of the unfolding reaction at high denaturant concentration, the acceleration of the refolding reaction at low denaturant concentration and the maximum relaxation time (minimum rate constant) near the midpoint of the transition.

The chevron analysis can provide several useful insights into folding mechanisms. First, the unfolding and refolding phases that connect smoothly with each other in the transition zone reflect a reversible folding reaction that limits both unfolding and refolding. If two or more chevrons are observed, vertically displaced from each other, a parallel channel folding mechanism is possible. Second, the denaturant dependences of the unfolding and refolding relaxation times provide information on the associated structural changes. Reactions that result in major changes in buried surface area display strong denaturant dependences of the relaxation times. Those that conserve the buried surface area, i.e. conformational rearrangements or that are limited by *cis*/*trans* proline isomerization, display little or no dependence on the denaturant concentration. Third, if the native thermodynamic state is comprised of two or more slowly interconverting forms, then the amplitudes of the several observed (potentially parallel) unfolding reactions would be expected to correlate closely with the relative populations of the multiple native conformers. The independent detection of multiple, slowly interconverting native conformers with techniques such as nuclear magnetic resonance (NMR) spectroscopy or pre-steady state ligand-binding experiments would provide support for such a conclusion. A lack of proportionality between the relative relaxation times and the relative amplitudes for the different events is consistent with a parallel folding mechanism. By contrast, a proportional relationship between the relaxation times and the amplitudes of the phases implies that a single species partitions into multiple product forms that could form the basis for subsequent parallel reactions. Fourth, if the sum of the absolute values of the denaturant dependences of the unfolding and refolding rate constants, i.e. the denaturant dependence of the transition state (‡) ($m^{\ddagger}$) values, for all of the kinetic steps is equal to the denaturant dependence extracted from the equilibrium data, the m_{eq} value, a sequential mechanism is possible. If the sum exceeds the equilibrium m_{eq} value, a parallel channel mechanism is possible.

Chevron analysis may also be used to distinguish whether an intermediate is on- or off-pathway. The sign of the urea dependence for a relaxation time reflects the burial or exposure of surface area: a decrease in relaxation time with decreasing urea (a positive $m^{\ddagger}$-value) indicates the burial of surface area and a decrease in relaxation time with increasing urea (a negative $m^{\ddagger}$-value) suggests the exposure of surface area. αTS [42], cytochrome *c* [96] and BPTI [97] display a negative $m^{\ddagger}$-value for one of the relaxation times observed under strongly folding conditions, implying that the phase is controlled by the unfolding of an early, off-pathway intermediate.

3.4.2. Case study

Dihydrofolate reductase: DHFR is an α/β/α protein where the (mostly) parallel 8-stranded β sheet is flanked on either side by two α helices. The β-sheet topology defines two structurally distinct domains: an adenosine-binding domain common to most nucleotide-binding proteins and a discontinuous loop domain comprised of segments from both the amino- and carboxy-termini [98]. The thermodynamic properties and kinetic folding mechanism of ecDHFR have been studied in detail, using a variety of biophysical techniques [36–40,84,85,99,100]. The first detectable step in this

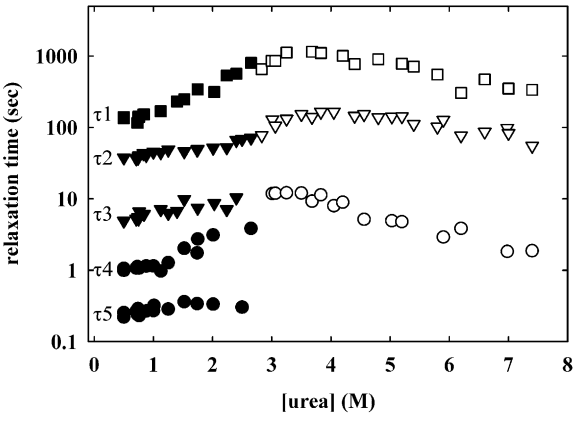

Fig. 3. The Chevron Analysis Test. *Chevron Plots:* urea dependence of the unfolding (open symbols) and refolding (closed symbols) relaxation times for 1 μM of ecDHFR at 15 °C. All phases were detected using Trp FL and the refolding phases are denoted τ1 through τ5 (in order of decreasing relaxation times). (Figure was used with permission from O'Neill (manuscript in preparation), see also Figure 3 in Ref. [38].)

complex reaction involves a rapid collapse (<5 ms) of the urea-denatured state to form a burst phase species (I_{BP}) that has significant secondary structure [40,99] and an exposed hydrophobic core [39]. The rapid establishment of the β-sheet topology is followed by the formation of a set of hyperfluorescent intermediate states (I_1–I_4; τ = 200 ms) that convert to the native states (N_1–N_4) via four parallel folding channels (relaxation times in the range of 1–100 s).

Chevron analysis of the unfolding and refolding kinetics of ecDHFR displayed a number of complexities (Fig. 3), some of which led to this kinetic model. The three slow unfolding phases (τ_1=300 s, τ_2=50 s; τ_3=8 s at 6.2 M urea) connect smoothly with three of the five refolding phases (τ_1=140 s; τ_2=50 s; τ_3=5 s at 0.76 M urea); these data are consistent with three reversible parallel unfolding and refolding reactions [25,38]. The relative amplitudes for the two major unfolding phases, t_1 and t_2, were approximately 0.2 and 0.8, very similar to the relative populations of a pair of native conformers that differ in ligand-binding properties [81,82]. This correlation suggests that the distinct native conformers result in separate unfolding pathways. The observation of the three complete chevrons suggests that the structural features that differentiate the channels arises early in folding and persist in the native conformations. The fastest observable refolding reaction, t_5, reflects the formation of a hyperfluorescent intermediate(s) that cannot bind a tight binding inhibitor, MTX. The t_4 reaction carries the bulk of the refolding protein (~60%), but leads to a native-like conformer (i.e. it binds MTX) that is not detectably populated at equilibrium under native conditions (no corresponding unfolding leg of the chevron). Because the relative amplitudes of the τ_1–τ_4 refolding reactions are not proportional to the relative relaxation times, the splitting into parallel channels must have occurred prior to the formation of a set of hyperfluorescent intermediates, i.e. in the unfolded state or in the burst phase reaction. HX-NMR experiments have demonstrated that at least two conformations are present after 13 ms of folding: a major species that protects a number of backbone amides against exchange and a minor species that does not [40].

3.4.3. Other studies

The folding kinetics for barstar, a small ribonuclease inhibitor, provides a variation on the parallel channels folding model [66,101,102]. This system has been extensively studied over the microsecond to minutes time range as a function of pH, GdmCl and urea [101]. The unfolded state exists as two forms; 30% that folds rapidly to the native state (U_f) and 70% that folds slowly (U_s). U_f is proposed to have Tyr47-Pro48 in the native *cis* conformation and U_s has the non-native *trans* isomer [103]. The unfolding and the refolding of barstar is therefore characterized by multiple intermediates and competing pathways. Both unfolded forms fold to the native state via an on-pathway compact premolten globule intermediate; U_f folds by only one pathway whereas the folding of U_s (under strongly stabilizing conditions, i.e. low denaturant concentrations) is proposed to occur via alternate and hence competing pathways. Isomerization about the crucial Xaa-Pro bond transforms the late intermediates to the native state. The presence of competing unfolding pathways, i.e. where a potentially sequential reaction is split into multiple parallel channels, and multiple intermediates was

suggested by three observations: (1) three probes, far-UV CD, FL and chemical modification, yielded different relaxation times for unfolding; (2) the denaturant dependence of the rate constants were different for each of the three probes; and (3) different responses in the burst phase. Recently, competing pathways have also been proposed for the pH-induced unfolding and refolding of barstar [102].

3.5. The Double-Jump Test

Double-jump experiments are widely used to monitor the time dependence of the population of multiple stable native, intermediate, and unfolded forms. They can also be used to discriminate between sequential and parallel folding mechanisms. Double-jump refolding (N → U → delay → N) and double-jump unfolding assays (U → N → delay → U) provide a means to detect the presence of slow interconverting unfolded [86] and native state populations [104], respectively.

3.5.1. Approach

Double-jump refolding assays: These assays exploit the fact that, immediately after unfolding, all molecules have all their peptidyl bonds in their native isomeric form. Successful application of this assay requires that the native protein unfold faster than either interconversions between multiple native forms if present or the subsequent interconversions between the multiple unfolded forms. Because this interconversion can require between 10 and 1000 s at room temperature for proline isomerization [105], strongly unfolding conditions are usually chosen. After various delay times at high denaturant concentration, aliquots are withdrawn and quickly transferred into native conditions to initiate refolding. After short unfolding times, most of the unfolded protein will refold rapidly. As the delay time increases, the amplitude for the slower refolding event will increase until equilibrium is achieved between the fast and slow unfolded species under unfolding conditions. The plot of the amplitudes of the folding reactions vs. the unfolding delay time can be fit to an exponential whose relaxation time reflects the formation of the alternative unfolded form. This assay has been applied to a number of proteins (e.g. RNase T1 [106,107], staphylococcal nuclease [108], thioredoxin [109], RNase A [110,111], αTS [42], and cytochrome *c* [65] and see review [112]).

Double-jump unfolding assays: A variation on the double-jump refolding assay provides a test for a sequential folding intermediate and permits an assessment of the heterogeneity of the native state that may result in parallel unfolding reactions. In these assays, the refolding of unfolded protein is initiated by dilution of denaturant. After various delay times, an aliquot is injected into strongly unfolding conditions and the amplitude of the unfolding phase(s) is measured. A lag phase in the appearance of the amplitude of the phase corresponding to the unfolding of the native protein implies a mandatory intermediate on a sequential pathway [67]. For proteins whose native state displays multiple unfolding phases, the progressive increase in the amplitudes of these phases at increasing delay times can be fit to exponential functions that reflect interconversions between multiple native or intermediate forms [42] or multiple, independent routes to a single native conformation [49].

3.5.2. Case study

E. coli Trp repressor: Homodimeric TR is a member of the helix–turn–helix DNA-binding protein family. Each monomer is composed of six α helices, some of which intertwine with those from the partner subunit to form the hydrophobic dimerization domain. The dimerization sequence is comprised of the A, B and C helices, the D and E helices form the DNA-reading heads and the terminal F helix pack against helices A and B of the partner subunit. The determination of a minimal folding mechanism of TR required a variety of approaches [44–49]. Although the urea-induced folding of TR is a reversible two-state equilibrium process [44], the folding mechanism is very complex.

The earliest folding event displays a burst phase in SF-CD and FL-detected 8-anilino-1-napthalenesulfonate (ANS)-binding that corresponds to the formation of a pair of partially folded monomeric intermediates. These two conformers were proposed to pair randomly via second-order reactions

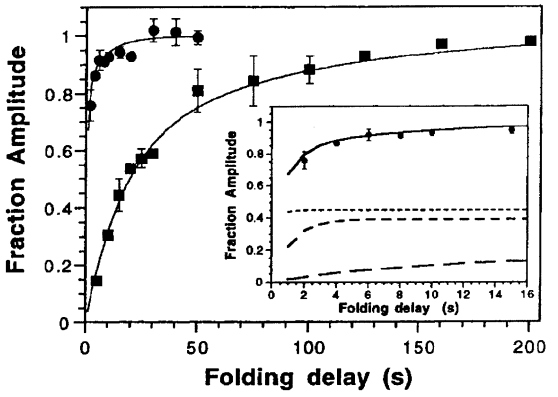

Fig. 4. The Double-Jump Test. *Manual-mixing double-jump experiments:* unfolded TR was refolded to 2.0 M (●) and 4.5 M (■) urea and 4.6 μM monomer. After various refolding delay times, the protein was unfolded to final conditions of 6.5 M urea and 2 μM monomer. The unfolding reaction was monitored using FL emission at 360 nm. *Inset:* Enlargement of the 2.0 M urea data at short refolding delay times. (Reprinted from Ref. [49], by permission of the publisher Academic Press.)

to form three dimeric intermediates that independently proceed via parallel channels to the native dimeric species. Neither the channels nor the three urea-independent rearrangement reactions that limit folding at low denaturant concentration reflect proline isomerization [46].

Double-jump unfolding assays [49] were used to monitor the formation of the native dimer, thereby testing the validity of the parallel folding mechanism. The presence of three folding reactions required that the double-jump assays be performed by refolding to 2.0 M urea, to highlight the fast and intermediate refolding phases, and at 4.5 M urea, to highlight the intermediate and slow folding phases (Fig. 4). The observed unfolding relaxation time was always equivalent to that for the unfolding of the native dimer to 6.5 M urea, implying that all three folding channels result in the formation of the native dimer. Simulations of the recovery of the unfolding amplitude expected for folding through three independent channels agreed with the experimental data, demonstrating that all three folding phases contribute independently to the formation of the native dimer.

3.6. The Ligand-Binding Test

3.6.1. Approach

The application of native-state ligands to probe folding reactions has provided compelling evidence to differentiate between sequential and parallel mechanisms. In this test, the refolding kinetics are monitored at varying ligand concentrations. The success of this test can be enhanced if several criteria are met: (1) ligand binding is rapid (i.e. occurs within the deadtime of SF mixing, <5 ms) so that the spectroscopic observations reflect folding, not ligand-binding reactions; (2) the ligand binds specifically to the native state with high affinity (low μM or nM range) to enable saturation at reasonable ligand concentrations; (3) the binding of the ligand can be monitored at a wavelength that can be discriminated from the optical properties of the protein so that the signal exclusively reflects the local environment of the ligand; and (4) the presence of the ligand should not perturb the folding mechanism, i.e. the relative amplitudes and relaxation times of the phases should be identical to those obtained using alternate probes for folding in the absence of the ligand.

This test involves monitoring the optical properties of the ligand during refolding as a function of the relative concentrations of ligand and protein. For a strictly sequential mechanism, ligand binding will be controlled by the final, rate-limiting step that produces the native conformation. If ligand is capable of binding to partially folded forms, complex kinetics may be observed. For a parallel mechanism, ligand binding may reveal complex kinetics that reflects the formation of multiple native or native-like forms capable of binding the ligand. The sequential and parallel possibilities can be discriminated with substoichiometric ligand concentration. For the sequential mechanism, the amplitudes of all of the refolding phases should be reduced in proportion to the fractional saturation. For the parallel mechanism, substoichiometric ratios of ligand/protein would lead to a selective loss of the amplitudes of the slow folding phases. This selective response reflects the binding of the ligand by the faster folding species, thereby reducing or eliminating the supply of ligand for the slower folding species.

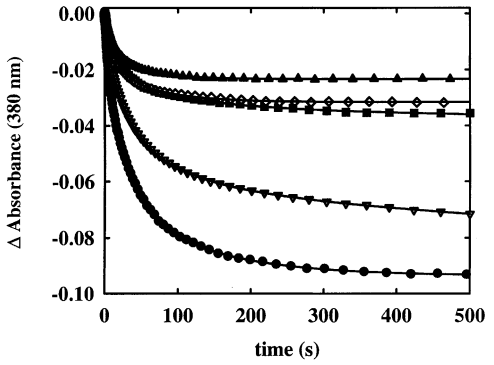

Fig. 5. The Ligand-Binding Test. Abs-detected changes observed at 380 nm (MTX-binding to DHFR) during the refolding of 16 μM lcDHFR from 4.5 to 0.75 M urea in the presence of various amounts of MTX. The solid lines represent the best fit to a lag phase and four exponentials, respectively. The MTX:lcDHFR ratios are 1.1:1 (●), 0.8:1 (▽), 0.6:1 (■), 0.5:1 (◇), 0.3:1 (▲). (Reprinted from Ref. [72], by permission of the publisher Academic Press.)

Schmid and Blaschek [113] first used this approach for studying RNase A by exploiting the tight binding properties of the specific inhibitor, cytidine phosphate (2′CMP). The Abs changes at 254 nm upon 2′CMP binding were used to monitor the slow folding kinetics of RNase A (the protein has an isoabsorbance point at this wavelength). At stoichiometric or greater concentrations of ligand, all folding events were observed. However, as the ligand concentration was decreased, there was a selective loss in the slower folding events.

3.6.2. Case study

dihydrofolate reductase: MTX binds to DHFR in the millisecond time range with nanomolar dissociation constant [114]. This tight binding competitive inhibitor has provided an excellent probe for monitoring the folding kinetics of DHFR ([38,72] and Section 3.2). Refolding of lcDHFR in the presence of stoichiometric amounts of MTX (Fig. 5) illustrates that the folding relaxation times are similar to those obtained using Trp FL. However, as the concentration of MTX was decreased, there was a selective loss of the slower folding phases. At a ratio of 0.3 mol of MTX to 1 mol of lcDHFR, no further changes in Abs at 380 nm occur after ∼40 s. These data are consistent with the expectations of a parallel channel folding mechanism (see above).

3.7. HX-NMR/MS Pulse-Labeling Test

3.7.1. Approach

A number of reviews on the application of pulse-labeling HX combined with mass spectrometry (MS) or NMR in elucidating protein-folding mechanisms are available [74–79]. The HX approach derives from the observation that the rate of solvent exchange of labile backbone and some side chain amide protons is dependent on their individual environments. In particular, amide protons in the native protein that exchange at much slower rates than predicted for unstructured peptides reflect their involvement in intramolecular hydrogen bonds (and hence secondary structure). Burial from solvent within the hydrophobic core is occasionally the dominant determinant of protection from exchange.

Briefly, in this method a fully deuterium-exchanged, unfolded protein is refolded for various lengths of time before a short pulse of H_2O at alkaline pH is given. After a pulse time sufficient to exchange solvent-exposed amide protons (usually <20 ms), the pH is rapidly neutralized, and the protein is allowed to fold to the native conformation. The ^{1}H-^{15}NHSQC spectrum of the protein reveals the stage of folding at which a particular amide proton is protected from exchange. HX-MS provides complementary information on the mass labeling of the entire protein during folding. The HX-NMR and/or HX-MS test have provided insight into the development of secondary structure during the folding of proteins such as cytochrome *c* [74], lysozyme [34,35,115]; barnase [116], DHFR [40], and IL-1β [73,80].

3.7.2. Case study

Hen egg white lysozyme: Lysozyme is a 129 residue monomeric protein with two structurally distinct domains: one largely α helical (the α-domain) and the other containing significant regions of β-sheet (the β-domain). Although the equilibrium unfolding of lysozyme is a two-state process with no significantly populated intermediates, the folding mechanism is complex. The two

major refolding tracks to the native state, detected using a variety of spectroscopic techniques, are denoted fast ($\tau \sim 100$ ms; 25–30%) and slow ($\tau \sim 300$ ms; 70– 75%). Approximately 10% of unfolded lysozyme folds very slowly ($\tau = 20$ s) by a reaction that is limited by proline isomerization [117]. Typically the folding reactions described for lysozyme refer only to those molecules not limited by prolyl isomerization [35,104].

HX-NMR and electrospray mass spectrometry (ES-MS) were powerful in providing a detailed view of the development of stable structure throughout lysozyme [34,115]. The data showed that the amide protons in both domains show biphasic protection (Fig. 6a). The fast phase has a time constant of 5–10 ms for each domain and an average amplitude of 40 and 25% for the α- and β-domain, respectively. The slow phases have average amplitudes and relaxation times of 45% and 65 ms, and 55% and 350 ms for the α- and the β-domain, respectively. This behavior suggests the presence of multiple folding pathways. The amplitudes and the time scales of the reactions indicate that *cis/trans* proline isomerization is not the source of the partitioning into parallel channels.

The NMR analysis of the HX labeling provides residue-specific information but does not reveal whether the two domains are formed cooperatively. HX combined with ES-MS was used to distinguish whether the fast phase results from the independent or the concerted folding of the two domains. The distribution of the masses in the samples generated in the HX experiments was monitored (Fig. 6b). Three well-defined species with different masses, and hence different degrees of protection were detected. One species displayed a mass between those observed for the denatured (low mass) and native (high mass) states. Both its mass and kinetic behavior suggest that this species should be associated with the major folding intermediate in which the α-domain is structured in the absence of a stable β-domain. This peak reached a maximum intensity at a refolding time of approximately 100 ms. The intensity of this peak does not decrease to less than 10% until approximately 1000 ms, which is consistent with the slow phase of protection of amides in the β-domain. The ESI-MS data together with the refolding protection kinetics

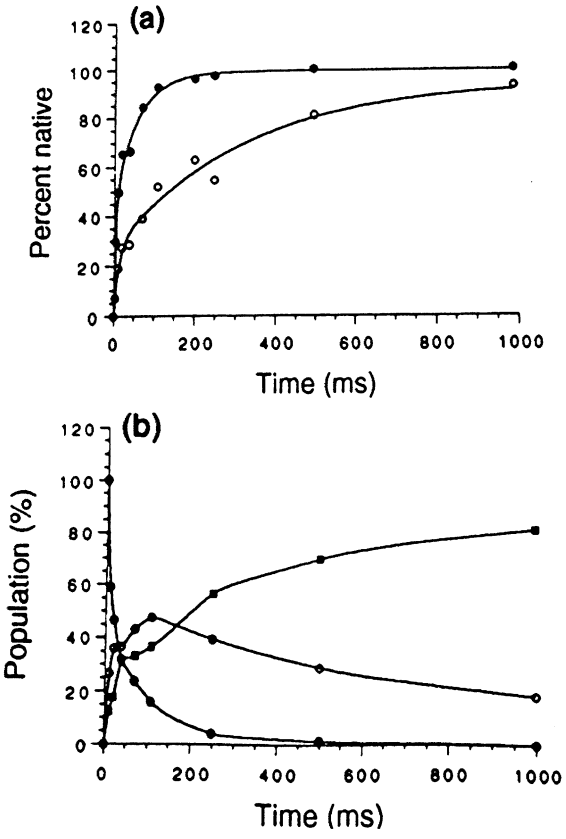

Fig. 6. HX-NMR/MS Pulse-labeling Test. The folding kinetics of lysozyme initiated by a 11-fold dilution (pH 5.5) from 6 M GdmCl at 20 °C. (a) HX labeling and two-dimensional NMR; average protection of the amides in the α- (●) and β- (○) domain is shown. (b) HX labeling and ESMS; unprotected state (●); species substantially protected only in the α-domain (○); species with native-like protection (■). (Reprinted from Ref. [35], with permission from Elsevier Science.)

observed using NMR suggest that the peak can be assigned to a species in which the α, but not the β, domain is protected from exchange. The identification of the species as an intermediate allowed the proposal of a parallel folding model for lysozyme where the structural domains may serve as distinct folding domains. The similar rates of the protection of different amides within each domain suggest that the formation of each domain is a highly cooperative process.

The observation of biphasic protection kinetics is explained by either (1) a partial protection of a

particular amide in all molecules or (2) complete protection but in only a proportion of molecules. The first scenario implies the sequential formation of a marginally stable intermediate followed by a slower transformation into a more stable, native-like state. The second scenario implies parallel pathways where one population of molecules folds rapidly to a fully protected structure and the other folds via a slower route. These two scenarios may be distinguished from each other by changing the pH of the pulse labeling solution [74,75,118]. If the extent of labeling of the majority of the amides does not depend significantly on the pH then the parallel channel mechanism is more likely. The partial protection offered by an intermediate on a sequential pathway is expected to be more sensitive to the enhanced exchange reaction at alkaline pH.

4. Perspective

Determining the mechanisms of folding reactions requires a combination of spectroscopic methods and classical experimental tests. With the exception of a few small proteins that fold in a simple two-state manner, folding mechanisms have proved to be surprisingly complex. Multiple pathways describe the folding of a number of systems, and the molecular basis for the origin of the different pathways has been explored. Alternate pathways may result from (i) *cis/trans* proline isomerization at the level of the unfolded protein as shown for cytochrome *c* [65,68], RNase A [111,119,120], RNase T1 [107], SNase [121], and αTS [42]; (ii) multiple native or native-like forms as shown for RNase A [113], DHFR [84,85], and H-ras p21 [122]; (iii) alternative docking modes for individual domains or different secondary structural elements as shown for lysozyme [35], TR [49], and proposed for DHFR [38,72]; (iv) non-native ligation states as observed for cytochrome *c* [96,123]; and (v) alternate disulphide bond formation as shown for BPTI [97,124] and insulin [125].

It is noteworthy that for some multimeric protein systems, e.g. the antibody domain C_H3 [126], the glutathione transferases [127] and TR [44,49], the observation of more than one second-order association step for a dimeric system was most easily explained by parallel folding pathways. Although the majority of folding studies are for water-soluble proteins, parallel folding pathways have been reported for the membrane protein bacteriorhodopsin [128]. The multiple folding routes for bacteriorhodopsin are pH dependent, implying that the routes arise from different protonation states of the protein.

The complex responses observed in unfolding and folding reactions of many proteins demonstrate the corresponding complexities of the underlying energy surfaces. Sequential mechanisms involve partially folded forms that may be crucial for rapid folding. Parallel mechanisms show that there can be more than one way for a protein to achieve its native conformation. An appreciation for the multidimensional nature of the reaction coordinate for protein-folding reactions, combined with the simple, organizing principles of chemical kinetics provides the perspectives and tools that may eventually lead, along with developments in theoretical and computational methods, to the solution of the protein-folding problem.

Acknowledgments

We are very pleased to recognize the many contributions that Prof. John Schellman has made to molecular biophysics over the past 50 years. His penetrating insights into fundamental issues have had a great impact on the approaches that we and others have adopted to solve the protein-folding problem. We stand on the broad shoulders of those who have gone before us to see more clearly into the future. Financial support for this work was provided by the National Science Foundation Grant MCB-0081076 and by the National Institutes of Health Grants GM54836 and GM23303 to C.R.M. We thank Drs Osman Bilsel, William R. Forsyth and Jill A. Zitzewitz for critically reading this manuscript. The authors also thank Drs John O'Neill, Jr. and Ying Wu for sharing and communicating unpublished data.

References

[1] C.B. Anfinsen, Principles that govern the folding of protein chains, Science 181 (1973) 223–230.

[2] C. Levinthal, Are there pathways for protein folding?, J. Chem. Phys. 65 (1968) 44–45.
[3] B. Honig, Protein folding: from the Levinthal paradox to structure prediction, J. Mol. Biol. 293 (1999) 283–293.
[4] C.R. Matthews, Pathways of protein folding, Annu. Rev. Biochem. 62 (1993) 653–683.
[5] K.A. Dill, H.S. Chan, From Levinthal to pathways to funnels, Nature Struct. Biol. 4 (1997) 10–19.
[6] C.M. Dobson, A. Sali, M. Karplus, Protein folding: a perspective from theory and experiment, Angew. Chem. Int. Ed. 37 (1998) 868–893.
[7] E. Alm, D. Baker, Matching theory and experiment in protein folding, Curr. Opin. Struct. Biol. 9 (1999) 189–196.
[8] R.L. Baldwin, G.D. Rose, Is protein folding hierarchic? I. Local structure and peptide folding, Trends Biochem. Sci. 24 (1999) 26–33.
[9] R.L. Baldwin, G.D. Rose, Is protein folding hierarchic? II. Folding intermediates and transition states, Trends Biochem. Sci. 24 (1999) 77–83.
[10] C.M. Dobson, M. Karplus, The fundamentals of protein folding: bringing together theory and experiment, Curr. Opin. Struct. Biol. 9 (1999) 92–101.
[11] A.R. Dinner, A. Sali, L.J. Smith, C.M. Dobson, M. Karplus, Understanding protein folding via free-energy surfaces from theory and experiment, Trends Biochem. Sci. (2000) 331–339.
[12] O. Bilsel, C.R. Matthews, Barriers in protein folding reactions, Adv. Prot. Chem. 53 (2000) 153–207.
[13] A.A. Frost, R.G. Pearson, Kinetics and Mechanism, Wiley, New York, 1961.
[14] H.A. Kramers, Brownian motion in a field of force and the diffusion model of chemical reactions, Physica 7 (1940) 284–304.
[15] S. Glasstone, K.J. Laidler, H. Eyring, Theory of the Rate Processes, McGraw-Hill, New York, 1940.
[16] P.G. Wolynes, J.N. Onuchic, D. Thirumalai, Navigating the folding routes, Science 267 (1995) 1619–1620.
[17] J.D. Bryngelson, J.N. Onuchic, N.D. Socci, P.G. Wolynes, Funnels, pathways, and the energy landscape of protein folding: a synthesis, Proteins Struct. Funct. Genet. 21 (1995) 167–195.
[18] J.N. Onuchic, H. Nymeyer, A.E. Garcia, J. Chahine, N.D. Socci, The energy landscape theory of protein folding: insights into folding mechanisms and scenarios, Adv. Protein Chem. 53 (2000) 87–152.
[19] R.L. Baldwin, On-pathway versus off-pathway folding intermediates, Fold. Des. 1 (1996) R1–R8.
[20] R.L. Baldwin, Competing unfolding pathways, Nature Struct. Biol. 4 (1997) 965–966.
[21] V.S. Pande, A.Y. Grosberg, T. Tanaka, D.S. Rokhsar, Pathways for protein folding: is a new view needed?, Curr. Opin. Struct. Biol. 8 (1998) 68–79.
[22] R. Zwanzig, Two-state models of protein folding kinetics, Proc. Natl. Acad. Sci. USA 94 (1997) 148–150.
[23] J. Sabelko, J. Ervin, M. Gruebele, Observation of strange kinetics in protein folding, Proc. Natl. Acad. Sci. USA 96 (1999) 6031–6036.
[24] C. Tanford, Protein denaturation, Adv. Protein Chem. 23 (1968) 121–282.
[25] C. Tanford, Protein denaturation. C. Theoretical models for the mechanism of denaturation, Adv. Protein Chem. 24 (1970) 1–95.
[26] A. Ikai, C. Tanford, Kinetics of unfolding and refolding of proteins I. Mathematical analysis, J. Mol. Biol. 73 (1973) 145–163.
[27] P.S. Kim, R.L. Baldwin, Intermediates in the folding reactions of small proteins, Annu. Rev. Biochem. 59 (1990) 631–660.
[28] S.E. Jackson, How do small single-domain proteins fold?, Fold. Des. 3 (1998) R81–R91.
[29] T. Schindler, M. Herrler, M.A. Marahiel, F.X. Schmid, Extremely rapid folding in the absence of intermediates, Nature Struct. Biol. 2 (1995) 663–673.
[30] K.L. Reid, H.M. Rodriguez, B.J. Hillier, L.M. Gregoret, Stability and folding properties of a model beta-sheet protein *Escherichia coli* CspA, Protein Sci. 7 (1998) 470–479.
[31] S.E. Jackson, A.R. Fersht, Folding of chymotrypsin inhibitor 2. 1. Evidence for a two-state transition, Biochemistry 30 (1991) 10428–10435.
[32] P.J. Hagerman, R.L. Baldwin, A quantitative treatment of the kinetics of the folding transition of ribonuclease A, Biochemistry 15 (1976) 1462–1473.
[33] K. Kuwajima, A folding model of alpha-lactalbumin deduced from the three-state denaturation mechanism, J. Mol. Biol. 114 (1977) 241–258.
[34] S.E. Radford, C.M. Dobson, P.A. Evans, The folding of hen lysozyme involves partially structured intermediates and multiple pathways, Nature 358 (1992) 302–307.
[35] C.M. Dobson, P.A. Evans, S.E. Radford, Understanding how proteins fold: the lysozyme story so far, Trends Biochem. Sci. 19 (1994) 31–37.
[36] N.A. Touchette, K.M. Perry, C.R. Matthews, Folding of dihydrofolate reductase from *Escherichia coli*, Biochemistry 25 (1986) 5445–5452.
[37] C. Frieden, Refolding of *Escherichia coli* dihydrofolate reductase: sequential formation of substrate binding sites, Proc. Natl. Acad. Sci. USA 87 (1990) 4413–4416.
[38] P.A. Jennings, B.E. Finn, B.E. Jones, C.R. Matthews, A reexamination of the folding mechanism of dihydrofolate reductase from *Escherichia coli:* verification and refinement of a four-channel model, Biochemistry 32 (1993) 3783–3789.
[39] B.E. Jones, P.A. Jennings, R.A. Pierre, C.R. Matthews, Development of nonpolar surfaces in the folding of *Escherichia coli* dihydrofolate reductase detected by 1-anilinonaphthalene-8-sulfonate binding, Biochemistry 33 (1994) 15250–15258.
[40] B.E. Jones, C.R. Matthews, Early intermediate in the folding of dihydrofolate reductase from *Escherichia coli*

detected by hydrogen exchange and NMR, Protein Sci. 4 (1995) 167–177.
[41] M.M. Crisanti, C.R. Matthews, Characterization of the slow steps in the folding of the α subunit of tryptophan synthase, Biochemistry 20 (1981) 2700–2706.
[42] O. Bilsel, J.A. Zitzewitz, K.E. Bowers, C.R. Matthews, Folding mechanism of the alpha-subunit of tryptophan synthase, an α/β barrel protein: global analysis highlights the interconversion of multiple native, intermediate, and unfolded forms through parallel channels, Biochemistry 38 (1999) 1018–1029.
[43] J.A. Zitzewitz, P.J. Gualfetti, I.E. Perkons, S.A. Wasta, C.R. Matthews, Identifying the structural boundaries of independent folding domains in the α/β barrel protein, α tryptophan synthase, Protein Sci. 8 (1999) 1200–1209.
[44] M.S. Gittelman, C.R. Matthews, Folding and stability of Trp aporepressor from *Escherichia coli*, Biochemistry 29 (1990) 7011–7020.
[45] C.J. Mann, C.R. Matthews, Structure and stability of an early folding intermediate of *Escherichia coli* Trp aporepressor measured by far-UV stopped-flow circular dichroism and 8-anilino-1-naphthalene sulfonate binding, Biochemistry 32 (1993) 5282–5290.
[46] C.J. Mann, X. Shao, C.R. Matthews, Characterization of the slow folding reactions of Trp aporepressor from *Escherichia coli* by mutational analysis of prolines and catalysis by a peptidyl–prolyl isomerase, Biochemistry 34 (1995) 14573–14580.
[47] L.M. Gloss, C.R. Matthews, Mechanism of folding of the dimeric core domain of *Escherichia coli* Trp repressor: a nearly diffusion-limited reaction leads to the formation of an on-pathway dimeric intermediate, Biochemistry 37 (1998) 15990–15999.
[48] L.M. Gloss, C.R. Matthews, The barriers in the bimolecular and unimolecular folding reactions of the dimeric core domain of *Escherichia coli Trp* repressor are dominated by enthalpic contributions, Biochemistry 37 (1998) 16000–16010.
[49] L.M. Gloss, B.R. Simler, C.R. Matthews, Rough energy landscapes in protein folding: dimeric *E. coli Trp* repressor folds through three parallel channels, J. Mol. Biol. 312 (2001) 1121–1134.
[50] A.C. Clark, S.W. Raso, J.F. Sinclair, M.M. Ziegler, A.F. Chaffotte, T.O. Baldwin, Kinetic mechanism of luciferase subunit folding and assembly, Biochemistry 36 (1997) 1891–1899.
[51] G. Wildegger, T. Kiefhaber, Three-state model for lysozyme folding: triangular folding mechanism with an energetically trapped intermediate, J. Mol. Biol. 270 (1997) 294–304.
[52] J. Fernandez-Recio, C.G. Genzor, J. Sancho, Apoflavodoxin folding mechanism: an α/β protein with an essentially off-pathway intermediate, Biochemistry 40 (2001) 15234–15245.
[53] H. Utiyama, R.L. Baldwin, Kinetic mechanisms of protein folding, Methods Enzymol. 131 (1986) 51–70.
[54] C.R. Matthews, Effect of point mutations on the folding of globular proteins, Methods Enzymol. 154 (1987) 498–511.
[55] M.R. Eftink, Use of multiple spectroscopic methods to monitor equilibrium unfolding of proteins, Methods Enzymol. 259 (1995) 487–512.
[56] M.C.R. Shastry, S.D. Luck, H. Roder, A continuous-flow capillary mixer to monitor reactions on the microsecond time scale, Biophys. J. 74 (1998) 2714–2721.
[57] H. Roder, M.R. Shastry, Methods for exploring early events in protein folding, Curr. Opin. Struct. Biol. 9 (1999) 620–626.
[58] P.A. Thompson, W.A. Eaton, J. Hofrichter, Laser temperature jump study of the helix-coil kinetics of an alanine peptide interpreted with a 'kinetic zipper' mode, Biochemistry 36 (1997) 9200–9210.
[59] M. Jacob, G. Holtermann, D. Perl, J. Reinstein, T. Schindler, M.A. Geeves, F.X. Schmid, Microsecond folding of the cold shock protein measured by a pressure-jump technique, Biochemistry 38 (1999) 2282–2891.
[60] K.A. Dill, D. Shortle, Denatured states of proteins, Annu. Rev. Biochem. 60 (1991) 795–825.
[61] C.N. Pace, B.A. Shirley, J.A. Thomson, Measuring the conformation stability of a protein, Protein Structure: A Practical Approach (1990) 311–330.
[62] J.A. Schellman, Solvent denaturation, Biopolymers 17 (1978) 1305–1322.
[63] B.A. Barshop, R.F. Wrenn, C. Frieden, Analysis of numerical methods for computer simulation of kinetic processes: development of KINSIM—a flexible, portable system, Anal. Biochem. 130 (1983) 134–145.
[64] Q. Dang, C. Frieden, New PC versions of the kinetic-simulation and fitting programs, KINSIM and FITSIM, Trends Biochem. Sci. 22 (1997) 317.
[65] J.J. Osterhout Jr., B.T. Nall, Slow refolding kinetics in yeast iso-2 cytochrome *c*, Biochemistry 24 (1985) 7999–8005.
[66] F.N. Zaidi, U. Nath, J.B. Udgaonkar, Multiple intermediates and transition states during protein unfolding, Nature Struct. Biol. 4 (1997) 1016–1024.
[67] F.X. Schmid, Mechanism of folding of ribonuclease A. Slow refolding is a sequential reaction via structural intermediates, Biochemistry 22 (1983) 4690–4696.
[68] M.M. Pierce, B.T. Nall, Coupled kinetic traps in cytochrome *c* folding: His-Heme misligation and proline isomerization, J. Mol. Biol. 298 (2000) 955–969.
[69] P.S. Kim, R.L. Baldwin, Specific intermediates in the folding reactions of small proteins and the mechanism of protein folding, Annu. Rev. Biochem. 51 (1982) 459–489.
[70] H. Roder, W. Colon, Kinetic role of early intermediates in protein folding, Curr. Opin. Struct. Biol. 7 (1997) 15–28.
[71] D.K. Heidary, J.C. O'Neill Jr., M. Roy, P.A. Jennings, An essential intermediate in the folding of dihydrofolate

reductase, Proc. Natl. Acad. Sci. USA 97 (2000) 5866–5870.
[72] L.A. Wallace, C.R. Matthews, Highly divergent dihydrofolate reductases conserve complex folding mechanisms, J. Mol. Biol. 315 (2002) 193–211.
[73] D.K. Heidary, L.A. Gross, M. Roy, P.A. Jennings, Evidence for an obligatory intermediate in the folding of interleukin-1 beta, Nature Struct. Biol. 4 (1997) 725–731.
[74] H. Roder, G.A. Elove, S.W. Englander, Structural characterization of folding intermediates in cytochrome *c* by H-exchange labelling and proton NMR, Nature 335 (1988) 700–704.
[75] J.B. Udgaonkar, R.L. Baldwin, NMR evidence for an early framework intermediate on the folding pathway of ribonuclease A, Nature 335 (1988) 694–699.
[76] H. Roder, Structural characterization of protein folding intermediates by proton magnetic resonance and hydrogen exchange, Methods Enzymol. 176 (1989) 446–473.
[77] T.M. Raschke, S. Marqusee, Hydrogen exchange studies of protein structure, Curr. Opin. Biotech. 9 (1998) 80–86.
[78] S.W. Englander, L. Mayne, Y. Bai, T.R. Sosnick, Hydrogen exchange: the modern legacy of Linderstom-Lang, Protein Sci. 6 (1997) 1101–1109.
[79] S.W. Englander, Protein folding intermediates and pathways studied by hydrogen exchange, Annu. Rev. Biophys. Biomol. Struct. 29 (2000) 213–238.
[80] P. Varley, A.M. Gronenborn, H. Christensen, P.T. Wingfield, R.H. Pain, G.M. Clore, Kinetics of folding of the all-beta sheet protein interleukin-1 beta, Science 260 (1993) 1110–1113.
[81] S.M. Dunn, J.G. Batchelor, R.W. King, Kinetics of ligand binding to dihydrofolate reductase: binary complex formation with NADPH and coenzyme analogues, Biochemistry 17 (1978) 2356–2364.
[82] S.M. Dunn, R.W. King, Kinetics of ternary complex formation between dihydrofolate reductase, coenzyme, and inhibitors, Biochemistry 19 (1980) 766–773.
[83] K. Taira, S.J. Benkovic, Evaluation of the importance of hydrophobic interactions in drug binding to dihydrofolate reductase, J. Med. Chem. 31 (1988) 129–137.
[84] C. Clarke, C. Frieden, Native *Escherichia coli* and murine dihydrofolate reductases contain late-folding non-native structures, J. Mol. Biol. 285 (1999) 1765–1776.
[85] R.M. Ionescu, V.F. Smith, J.C. O'Neill Jr., C.R. Matthews, Multistate equilibrium unfolding of *Escherichia coli* dihydrofolate reductase: thermodynamic and spectroscopic description of the native, intermediate, and unfolded ensembles, Biochemistry 39 (2000) 9540–9550.
[86] J.F. Brandts, H.R. Halvorson, M. Brennan, Consideration of the possibility that the slow step in protein denaturation reactions is due to *cis–trans* isomerism of proline residues, Biochemistry 14 (1975) 4953–4963.
[87] C.R. Matthews, M.M. Crisanti, J.T. Manz, G.L. Gepner, Effect of a single amino acid substitution on the folding of the a subunit of tryptophan synthase, Biochemistry 22 (1983) 1445–1452.
[88] M.R. Hurle, C.R. Matthews, Proline isomerization and the slow folding reactions of the α subunit of tryptophan synthase from *Escherichia coli*, Biochim. Biophys. Acta 913 (1987) 179–184.
[89] M.R. Hurle, G.A. Michelotti, M.M. Crisanti, C.R. Matthews, Characterization of a slow folding reaction for the α subunit of tryptophan synthase, Proteins Struct. Funct. Genet. 2 (1987) 54–63.
[90] N.B. Tweedy, M.R. Hurle, B.A. Chrunyk, C.R. Matthews, Multiple replacements at position 211 in the α subunit of tryptophan synthase as a probe of the folding unit association reaction, Biochemistry 29 (1990) 1539–1545.
[91] J.A. Zitzewitz, C.R. Matthews, Molecular dissection of the folding mechanism of the alpha subunit of tryptophan synthase: an amino-terminal autonomous folding unit controls several rate-limiting steps in the folding of a single domain protein, Biochemistry 38 (1999) 10205–10214.
[92] K. Ogasahara, K. Yutani, Unfolding–refolding kinetics of the tryptophan synthase alpha subunit by CD and fluorescence measurements, J. Mol. Biol. 236 (1994) 1227–1240.
[93] K. Ogasahara, K. Yutani, Equilibrium and kinetic analyses of unfolding and refolding for the conserved proline mutants of tryptophan synthase alpha subunit, Biochemistry 36 (1997) 932–940.
[94] C.R. Matthews, M.M. Crisanti, Urea-induced unfolding of the α subunit of tryptophan synthase: evidence for a multistate process, Biochemistry 20 (1981) 784–792.
[95] P.J. Gualfetti, O. Bilsel, C.R. Matthews, The progressive development of structure and stability during the folding of the a subunit of tryptophan synthase from *E. coli*, Protein Sci. 8 (1999) 1623–1635.
[96] T.R. Sosnick, L. Mayne, S.W. Englander, Molecular collapse: the rate-limiting step in two-state cytochrome *c* folding, Proteins Struct. Funct. Genet. 24 (1996) 413–426.
[97] J.S. Weissman, P.S. Kim, A kinetic explanation for the rearrangement pathway of BPTI folding, Nature Struct. Biol. 2 (1995) 1123–1130.
[98] M.R. Sawaya, J. Kraut, Loop and subdomain movements in the mechanism of *Escherichia coli* dihydrofolate reductase: crystallographic evidence, Biochemistry 36 (1997) 586–603.
[99] K. Kuwajima, E.P. Garvey, B.E. Finn, C.R. Matthews, S. Sugai, Transient intermediates in the folding of dihydrofolate reductase as detected by far-ultraviolet circular dichroism spectroscopy, Biochemistry 30 (1991) 7693–7703.
[100] J.C. O'Neill Jr., C.R. Matthews, Localized, stereochemically-sensitive hydrophobic packing in an early inter-

mediate of dihydrofolate reductase of *Escherichia coli*, J. Mol. Biol. 295 (2000) 737–744.
[101] M.C. Shastry, J.B. Udgaonkar, The folding mechanism of barstar: evidence for multiple pathways and multiple intermediates, J. Mol. Biol. 247 (1995) 1013–1027.
[102] B.R. Rami, J.B. Udgaonkar, pH-jump-induced folding and unfolding studies of barstar: evidence for multiple folding and unfolding pathways, Biochemistry 40 (2001) 15267–15279.
[103] G. Schreiber, A.R. Fersht, The refolding of *cis*- and *trans*-peptidylprolyl isomers of barstar, Biochemistry 32 (1993) 11195–11203.
[104] T. Kiefhaber, Kinetic traps in lysozyme folding, Proc. Natl. Acad. Sci. USA 92 (1995) 9029–9033.
[105] C. Grathwohl, K. Wuthrich, The X-Pro peptide bond as an NMR probe for conformational studies of flexible linear peptides, Biopolymers 15 (1976) 2025–2041.
[106] T. Kiefhaber, R. Quaas, U. Hahn, F.X. Schmid, Folding of ribonuclease T1. 1. Existence of multiple unfolded states created by proline isomerization, Biochemistry 29 (1990) 3053–3061.
[107] L.M. Mayr, C. Odefey, M. Schutkowski, F.X. Schmid, Kinetic analysis of the unfolding and refolding of ribonuclease T1 by a stopped-flow double-mixing technique, Biochemistry 35 (1996) 5550–5561.
[108] K. Kuwajima, N. Okayama, K. Yamamoto, T. Ishihara, S. Sugai, The Pro117 to glycine mutation of staphylococcal nuclease simplifies the unfolding–folding kinetics, FEBS Lett. 290 (1991) 135–138.
[109] R.F. Kelley, J. Wilson, C. Bryant, E. Stellwagen, Effects of guanidine hydrochloride on the refolding kinetics of denatured thioredoxin, Biochemistry 25 (1986) 728–732.
[110] R.W. Dodge, H.A. Scheraga, Folding and unfolding kinetics of the proline-to-alanine mutants of bovine pancreatic ribonuclease A, Biochemistry 35 (1996) 1548–1559.
[111] R.A. Sendak, D.M. Rothwarf, W.J. Wedemeyer, W.A. Houry, H.A. Scheraga, Kinetic and thermodynamic studies of the folding/unfolding of a tryptophan-containing mutant of ribonuclease A, Biochemistry 35 (1996) 12978–12992.
[112] F.X. Schmid, Fast-folding and slow-folding forms of unfolded proteins, Methods Enzymol. 131 (1986) 70–82.
[113] F.X. Schmid, H. Blaschek, A native-like intermediate on the ribonuclease A folding pathway. 2. Comparison of its properties to native ribonuclease A, Eur. J. Biochem. 114 (1981) 111–117.
[114] J.W. Williams, J.F. Morrison, R.G. Duggleby, Methotrexate, a high-affinity pseudosubstrate of dihydrofolate reductase, Biochemistry 18 (1979) 2567–2573.
[115] A. Miranker, S.E. Radford, M. Karplus, C.M. Dobson, Demonstration by NMR of folding domains in lysozyme, Nature 349 (1991) 633–636.
[116] M. Bycroft, A. Matouschek, J.T.J. Kellis, L. Serrano, A.R. Fersht, Detection and characterization of a folding intermediate in barnase by NMR, Nature 346 (1990) 488–490.
[117] S. Kato, N. Shimamoto, H. Utiyama, Identification and characterization of the direct folding process of hen egg-white lysozyme, Biochemistry 21 (1982) 38–43.
[118] J.B. Udgaonkar, R.L. Baldwin, Early folding intermediate of ribonuclease A, Proc. Natl. Acad. Sci. USA 87 (1990) 8197–8201.
[119] D.A. Schultz, F.X. Schmid, R.L. Baldwin, *Cis* proline mutants of ribonuclease A. II. Elimination of the slow-folding forms by mutation, Protein Sci. 1 (1992) 917–924.
[120] W.A. Houry, H.A. Scheraga, Nature of the unfolded state of ribonuclease A: effect of *cis–trans* X-Pro peptide bond isomerization, Biochemistry 35 (1996) 11719–11733.
[121] T. Ikura, G.P. Tsurupa, K. Kuwajima, Kinetic folding and *cis/trans* prolyl isomerization of staphylococcal nuclease. A study by stopped-flow absorption, stopped-flow circular dichroism, and molecular dynamics simulations, Biochemistry 36 (1997) 6529–6538.
[122] J. Zhang, C.R. Matthews, The role of ligand binding in the kinetic folding mechanism of human p21 (H-ras) protein, Biochemistry 37 (1998) 14891–14899.
[123] G.A. Elove, A.K. Bhuyan, H. Roder, Kinetic mechanism of cytochrome *c* folding: involvement of the heme and its ligands, Biochemistry 33 (1994) 6925–6935.
[124] T.E. Creighton, D.P. Goldenberg, Kinetic role of a metastable native-like two-disulphide species in the folding transition of bovine pancreatic trypsin inhibitor, J. Mol. Biol. 179 (1984) 497–526.
[125] Q.X. Hua, S.N. Gozani, R.E. Chance, J.A. Hoffmann, B.H. Frank, M.A. Weiss, Structure of a protein in a kinetic trap, Nature Struct. Biol. 2 (1995) 129–138.
[126] M.J.W. Thies, J. Mayer, J.G. Augustine, C.A. Frederick, H. Lillie, J. Buchner, Folding and association of the antibody domain C_H3: prolyl isomerization precedes dimerization, J. Mol. Biol. 293 (1999) 67–79.
[127] L.A. Wallace, H.W. Dirr, Folding and assembly of dimeric human glutathione transferase A1-1, Biochemistry 38 (1999) 16686–16694.
[128] H. Lu, P.J. Booth, The final stages of folding of the membrane protein bacteriorhodopsin occur by kinetically indistinguishable parallel folding paths that are mediated by pH, J. Mol. Biol. 299 (2000) 233–243.